

Design and operation of a fast, thin-film thermocouple probe on a turbine engine

Roger D. Meredith,^{*} John D. Wrbanek,[†] Gustave C. Fralick,[‡] Lawrence C. Greer III,[§] Gary W. Hunter^{**}
NASA Glenn Research Center, Cleveland, OH 44135

and

Liang-Yu Chen^{††}
Ohio Aerospace Institute, Brook Park, OH 44142

As a demonstration of technology maturation, a thin-film temperature sensor probe was fabricated and installed on a F117 turbofan engine via a borescope access port to monitor the temperature experienced in the bleed air passage of the compressor area during an engine checkout test run. To withstand the harsh conditions experienced in this environment, the sensor probe was built from high temperature materials. The thin-film thermocouple sensing elements were deposited by physical vapor deposition using pure metal elements, thus avoiding the inconsistencies of sputter-depositing particular percentages of materials to form standardized alloys commonly found in thermocouples. The sensor probe and assembly were subjected to a strict protocol of multi-axis vibrational testing as well as elevated temperature pressure testing to be qualified for this application. The thin-film thermocouple probe demonstrated a faster response than a traditional embedded thermocouple during the engine checkout run.

Nomenclature

α	=	thermal diffusivity ($\text{mm}^2 \cdot \text{s}^{-1}$)
$Au-Pt$	=	gold vs. platinum (as a thermocouple)
CTE	=	coefficient of thermal expansion ($\mu\text{m}/\text{m} \cdot \text{K}$)
dt	=	time step (s)
Δt	=	time increment (numerical modeling)
Δx	=	distance increment (numerical modeling)
EHM	=	Engine Health Management (system)
FFT	=	fast Fourier transform (analysis algorithm)
GRC	=	Glenn Research Center (in Cleveland, Ohio)
j, n	=	node, step indices (numerical modeling)
τ	=	thermal time constant, of a thermocouple (s)
$T(t)$	=	thermocouple reading ($^{\circ}\text{C}$)
$T_g(t)$	=	gas temperature ($^{\circ}\text{C}$)
\dot{T}	=	rate of heating, dT/dt , of a thermocouple ($^{\circ}\text{C}/\text{s}$)
$VIPR$	=	Vehicle Integrated Propulsion Research (project)

^{*} R&D Engineer, Smart Sensors and Electronics Systems, NASA GRC MS 77-1

[†] R&D Engineer, Smart Sensors and Electronics Systems, NASA GRC MS 77-1, AIAA Senior Member

[‡] R&D Senior Engineer, Smart Sensors and Electronics Systems, NASA GRC MS 77-1, AIAA Senior Member

[§] R&D Senior Engineer, Smart Sensors and Electronics Systems, NASA GRC MS 77-1

^{**} R&D Senior Engineer, Smart Sensors and Electronics Systems, NASA GRC MS 77-1, AIAA Senior Member

^{††} Senior Research Associate, Smart Sensors and Electronics Systems, NASA GRC MS 77-1

I. Introduction

THIN-FILM sensors are much less disturbing to the operating environment, have a minimal impact on the physical characteristics of the supporting components, and with much less mass than wires or foils, will react considerably faster to subtle transient effects. Advancements in thin-film sensor technology can be useful in engine diagnostics by providing data to closed-loop systems and to operators concerning engine stability or compressor instabilities. The dynamic nature of the thin-film sensor response provides real-time measurements with minimal intrusion into the area of interest, and provides data with much greater time resolution to uncover more subtle effects than standard thermocouple probes.

The Smart Sensors and Electronics Systems Branch of the NASA Glenn Research Center (GRC) has an in-house effort to develop thin-film sensors for surface measurements for propulsion system research.¹ The sensors of interest include those for measuring strain, temperature, heat flux and surface flow, which will enable critical vehicle health monitoring of future space and air vehicles. The use of sensors made of thin films does not require special machining of the components on which they are mounted, and with thicknesses less than 10 μm , they are considerably thinner than wire or foils.

The NASA Vehicle Integrated Propulsion Research (VIPR) project is an on-going ground-based engine test project that utilizes a Pratt & Whitney F117 turbofan² engine aimed at maturing Engine Health Management (EHM) technologies.³ One of the VIPR project's many objectives in 2013 was to acquire data from a thin-film thermocouple probe installed in the engine. Successful completion of this objective would establish a core capability for implementing thin-film sensor probes in harsh environments. This capability will yield new information for gas-path models as well as demonstrate the viability of thin-film sensor probes in an engine environment.

To demonstrate the thin-film thermocouple probe as a viable sensor in an operating engine environment, a sensor probe was designed for installation in a borescope port in the high-pressure compressor section of the test engine. Borescope ports have been used extensively in the past for evaluation of sensor technology and engine research. Installation in a borescope port is easily implemented and allows evaluation of a range of sensor technologies without modification to the engine.

Gold versus platinum (Au-Pt) as a thermocouple has been extensively characterized⁴ and utilized at GRC in the fabrication of a thin-film heat flux sensor to 960°C for a Stirling convertor.⁵ Given the VIPR test and qualification requirements for this sensor probe, a Au-Pt thin-film thermocouple was selected for demonstration because it has been shown to have very good stability and fewer problems bonding lead wires to the thin-film as compared to other high-temperature metals.

II. Thermocouple Probe Design and Fabrication

Typical thermocouple probes are either *grounded* such that the thermocouple junction is in electrical and thermal contact with the probe sheath, *ungrounded* such that the thermocouple junction is embedded into the sheath insulated by an oxide, or *exposed* such that the thermocouple junction is beyond the end of the sheath.

The exposed thermocouple type is considered the fastest due to the small amount of mass needed to change temperature for a reading, though dependent on the method of forming the junction (e.g., butt-weld, beaded). For constant heat transfer conditions, the time constant of a thermocouple is proportional to the cross section area of the junction, so exposed wire thermocouples are faster than the other probe types by the square of the fraction of the probe diameter to wire diameter. However, exposed thermocouples are unprotected and subject to wire damage when placed in a harsh environment such as a turbojet engine.

The grounded and ungrounded thermocouple probes are more resilient for harsh applications because no wires are exposed to the harsh environments. Of these two types, the ungrounded is slower because it has not only the tip of the probe to change temperature, but the insulation that the wire is embedded in as well. For this reason, the time constants for commercial ungrounded probes are typically given as 1.5 times as much as that of grounded probes.

The sensor tested for VIPR had both an embedded Type K ungrounded probe as well as an Au-Pt thin-film thermocouple on its surface. The thin-film thermocouple sensor probe was designed in unison with a borescope plug adapter for the F117 engine, a customized compression fitting welded to a replicated, bored-out borescope plug. Figure 1 shows a cross-section schematic of the sensor probe body with port plug, port compression fitting, and probe cap, modeled to show the sensor tip flush with the internal passage. The sensor body itself was fabricated from alloy 316 stainless steel bored out for the thin-film sensor lead wires to be cemented in place.

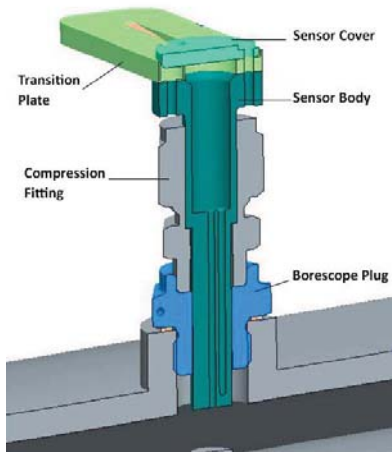


Figure 1. Cross-section schematic of the sensor body with port plug, compression fitting, cap and transition plate.

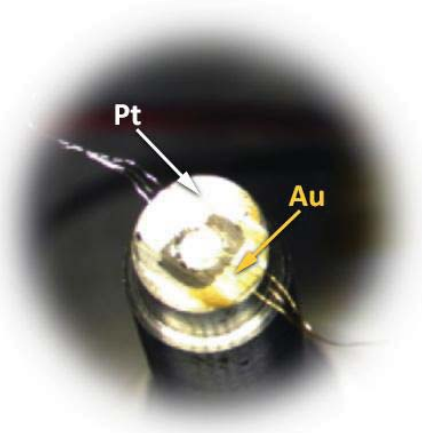


Figure 2. Fabricated probe tip showing platinum and gold thin films and lead wires ready for bonding to the films.

The Au-Pt thin films were sputter-deposited onto the tip of the sensor body and the lead wires bonded to the films. Wires of Au and Pt were used as lead wires, extending from the metal film through the sensor probe body. Figure 2 shows the sensor probe tip from a sensor with the Au and Pt thin films sputtered and lead wires ready for bonding to the films.

As mentioned above, the sensor probe was designed for insertion into a commercial ferruled compression tube fitting welded to a borescope port plug. At the compression ferrule, the sensor probe body was machined to replicate a stainless steel, half-inch diameter heavy wall tube to comply with the design of the commercial fitting. The sensor probe body was bored through, creating a path for 76 μm (0.003") diameter wires to pass internally from the tip to a transition plate on the back end, where they were terminated inside a high temperature commercial thermocouple connector. These wires were sleeved inside alumina (ceramic) tubes and beads, strain-relieved and potted with ceramic cement to fill the internal bore of the sensor probe body. The provision for an ungrounded metal-jacketed thermocouple was included in the internal bore.

The potting cement material was selected to best match the coefficient of thermal expansion (CTE) of the various materials, and internal details within the bore provided a locking mechanism for the cement. At operating temperature, the stainless steel body would grow at a faster rate than the cement and these steps mitigated the catastrophic failure of the cement due to CTE mismatch. At the sensor probe tip, the small wires were parallel gap welded to the deposited thin-film within a contoured surface. The welds were then over-coated with cement to support the connection during testing.

For comparison purposes, an ANSI-standard Type K thermocouple was embedded inside the sensor probe body, approximately a quarter inch from the thin-film deposition. A protective crown was welded over the tip to allow air to reach the film but to also prohibit the internal ceramic insulator tube from dislodging from the sensor probe body and damaging the engine if the sensor failed.

The outputs from the thin-film sensor and the embedded Type K thermocouple were converted to a temperature and digitized by a VIPR2 thermocouple data acquisition unit custom-designed and built at GRC. The resulting data stream was collected by a PC-based data acquisition system. The digitizer used an ANSI reference and an internal cold junction to determine the temperature readings.

III. VIPR2 Thermocouple Data Acquisition Unit

The VIPR2 thermocouple data acquisition unit (or digitizer) was designed to simultaneously acquire data from two thermocouples at a rate of 10 times per second. One of the two thermocouple acquisition ports was designed for Type K probes and the other was designed for either Type R or Au-Pt probes. Each thermocouple channel returns the raw thermocouple hot-junction temperature as well as its corresponding cold-junction temperature. Using this data, the cold-junction compensated millivolt output of each thermocouple probe is calculated.

Next, with the aid of NIST-derived conversion polynomials,^{4,6} the corresponding millivolt outputs of the cold junctions are calculated. The cold and hot junction voltages are summed for each probe and the summations are converted to temperatures from another set of NIST-derived conversion polynomials that yield temperatures accurate to within $\pm 0.06^\circ\text{C}$ over the entire operating range of the sensor. The VIPR2 thermocouple data acquisition unit utilizes a four-data-point wide sliding window for capturing the mean of the temperature data.

Two key design criteria for the VIPR2 thermocouple data acquisition unit are to maximize sensor accuracy and reduce signal noise. With this in mind, the VIPR2 thermocouple data acquisition unit was designed to digitize the sensor data as close to the sensor as possible and send data packets to a separate receiver unit over a RS-485 bus. A third design constraint, due to the anticipated proximity to the jet engine, mandates that all components used to build the VIP2 thermocouple data acquisition unit must operate within the extended temperature range of -40°C to $+125^\circ\text{C}$.

On the other hand, the receiver unit which possesses a LCD screen used to monitor the two thermocouple probes is constructed with standard commercial temperature parts due to the benign temperature environment near the test rack. The receiver unit also has a RS-232 port for communicating with a laptop PC running a GUI program that records and time stamps the temperature data to a user specified file. Lastly, the receiver unit has a clocked 8-bit wide parallel output bus that can be interfaced to a data acquisition rack, but was not connected in this demonstration.

The VIPR2 thermocouple data acquisition unit is built around a pair of automotive-grade thermocouple-to-digital conversion chips. These chips are optimized for a variety of thermocouple types and possess $\pm 2^\circ\text{C}$ accuracy over the entire Type K range and similar accuracies with other probe types. The hot-junction voltage is acquired using a 14-bit conversion and the cold-junction temperature is acquired using a 12-bit conversion.

To reduce signal noise, the sensor input is filtered using radio frequency interference-suppressing beads and capacitors. Serving as the core of the VIPR2 thermocouple data acquisition unit, the automotive-grade microcontroller acquires and processes data at a clock speed of 48MHz. The microcontroller drives the Serial Peripheral Interface bus serving as the master to two conversion chip slaves. In order to provide long distance serial communication, a pair of RS-485 line drivers is used to send data over 150 feet to the receiver module with its own matching pair of line drivers. The microcontroller also controls the LCD receiver module and uses its two universal asynchronous receiver/transmitter (UART) channels to send data from the remote sender to the receiver over the RS-485 lines and data to the PC over the RS-232 lines. Lastly, the microcontroller clocks data out over an 8-bit wide parallel port.

The firmware for the VIPR2 thermocouple data acquisition unit was written as a single program with a user selectable definition section to accommodate any of three incarnations of the board. Sections of code are included or excluded depending on the choices made with the configuration definitions. These major code sections are responsible for managing the SPI bus tied to the thermocouple-to-digital conversion chips, monitoring the two built-in UARTS for communication between the sender and receiver units as well as communication with the PC serial bus, handling the external 8-bit wide parallel port and controlling the LCD.

IV. Operational Test

After the sensor probe was fabricated, the package was subjected to a rigorous multi-axis vibration test schedule as well as a pressure at temperature test protocol prescribed by the VIPR test requirements and were performed at GRC. The qualifying conditions of the sensor were the survivability after 20g shock at room temperature and operation at 5,357 kPa (777 psia) at a maximum temperature of 633°C .

The operation of a thin-film thermocouple sensor probe prototype was validated during a *green run* checkout test of a pre-production F117-PW-100 turbofan² engine modified for the VIPR project. As a sanity check, the reliable operation of the probe in the planned validation configuration was verified by placing it inside a box furnace set to 150°C , noting the difference between the Au-Pt thin-film thermocouple and the embedded Type K thermocouple. The variation of the measured temperature by the probe against the calibrated embedded Type K thermocouple was on average 3°C low, and indicated a much faster time response of the thin-film thermocouple as compared to the embedded thermocouple. Though not a true calibration, the bench test provided confidence that the probe's thin-film thermocouple as connected to the VIPR2 thermocouple data acquisition unit performed to the expected $\pm 1^\circ\text{C}$ provided the offset of -3°C is taken into account.

The probe was installed in the F117 engine for the test using a borescope access port as show in Fig. 3, with the thin-film sensor element flush with the inner wall of the bleed air passage of the compressor at the area of interest. A schematic of the test arrangement is shown in Fig. 4. Data collected from the sensor tracked temperature changes

as the engine was cycled through multiple power settings, as shown in Fig. 5. The embedded Type K thermocouple tracked the temperature trend while the thin-film sensing element, which is positioned closer to the engine core, maintained a slightly higher reading during increased engine speed, but cooled at a faster rate when the engine performance was throttled back.

The temperature difference between the probe connector and the digitizer box was also monitored. There was a slight offset due to the temperature difference between these points, which was found to be between 2.0 — 3.0°C, essentially cancelling the -3°C offset found in the bench test to within the ±1°C of the reading.



Figure 3. Thermocouple probe installed in F117 turbofan engine.

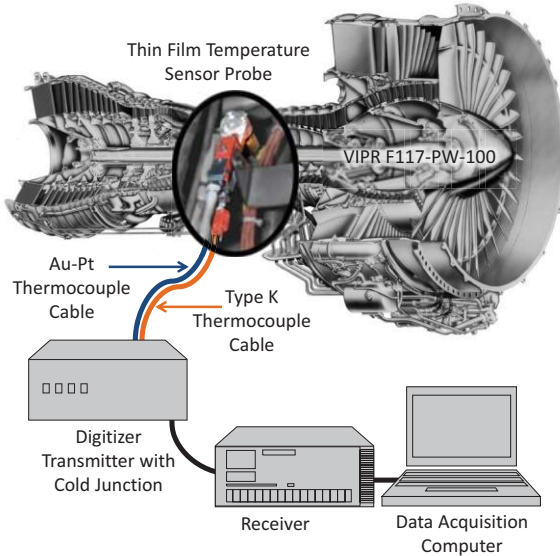


Figure 4. Thermocouple probe test schematic for F117 engine green run test.

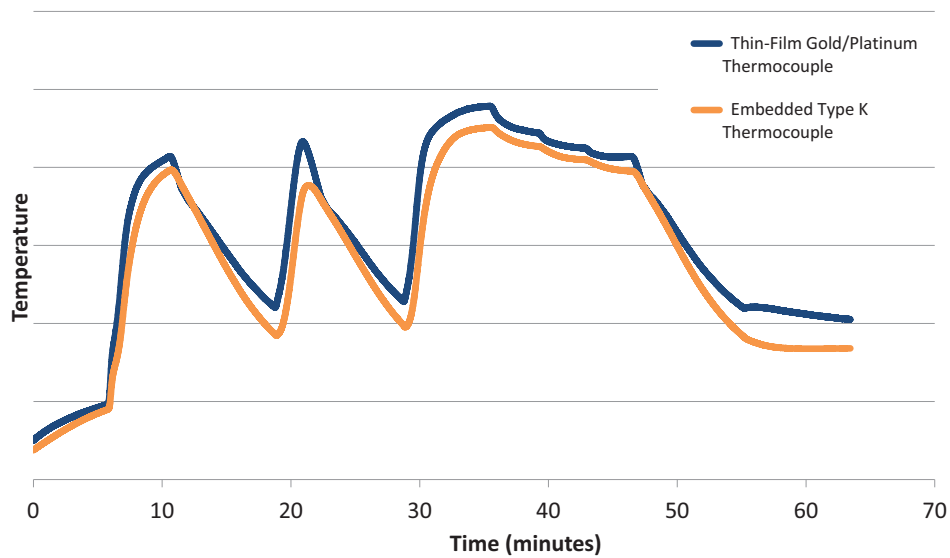


Figure 5. Thermocouple probe output from green run test showing relative thin-film and Type K thermocouple readings.

V. Results and Discussion

A. Multi-wire Analysis

Using the approach of multi-wire thermocouple probe analysis of Forney and Fralick,^{7,8} the thermal time constant for each thermocouple can be estimated by examining the measured temperatures from both the thin film and Type K thermocouples during the run. The thermal time constant (τ) is a ratio of the time dependent temperature difference from the gas temperature ($\{T_g(t)-T(t)\}$) to the rate of heating (or cooling) (dT/dt , or \dot{T}) as shown in Eq. (1).

$$dT/dt = (1/\tau) \cdot \{T_g(t)-T(t)\} \quad (1)$$

The challenge for the analysis of the green run data is that the gas temperature was unknown and changing with time as well. The time constants can be estimated by minimizing the difference of the gas temperature calculated by both thermocouples $\Delta T_g(t)$, which should ideally completely cancel as in Eq. (2).

$$T_g(t) = T_1(t) + \tau_1 \cdot \dot{T}_1$$

$$T_g(t) = T_2(t) + \tau_2 \cdot \dot{T}_2$$

$$T_1(t) - T_2(t) + \tau_1 \cdot \dot{T}_1 - \tau_2 \cdot \dot{T}_2 = 0 \quad (2)$$

The resulting gas temperature taking into account both thermocouple readings and time constants is found by dividing Eq. (1) for both thermocouples and solving for $T_g(t)$ as in Eq. (3).

$$T_g(t) = \frac{T_2 \left(\frac{\dot{T}_1}{\dot{T}_2} \right) - T_1 \left(\frac{\tau_2}{\tau_1} \right)}{\left(\frac{\dot{T}_1}{\dot{T}_2} \right) - \left(\frac{\tau_2}{\tau_1} \right)} \quad (3)$$

For our application, the size of the thermocouple probe eliminates sensitivity to high frequency effects much greater than 1 Hz, so the \dot{T} values were calculated over 1 second of data (8 data points) to reduce noise. The root mean square of the calculated ΔT_g summed over the data set was minimized to find the time constants. In this case, T_1 , \dot{T}_1 and τ_1 refer to the thin film thermocouple, and T_2 , \dot{T}_2 and τ_2 refer to the embedded Type K thermocouple.

As a consequence of the ratio of time constants in Eq. (3), the ratio τ_2/τ_1 was found in Eq. (2) through the mean square fitting, and then τ_2 was found. The time constants were determined to be 26.2 seconds for the Type K thermocouple and 2.40 seconds for the thin film thermocouple. As noted previously, the Type K thermocouple was embedded in a well offset from the centerline by 2.54 mm (0.100"), 8.76 mm (0.345") from the end of the sensor probe body, which led to the increased the response time.

B. Numerical Modeling Analysis

Numerically modeling the performance of the sensor probe allows an estimate of time constant based on the distance and the probe body material properties. Since the sensor probe tip is designed to be even with the inside wall of the bleed air chamber, a one-dimensional model is a sufficient approximation of the reaction time, reducing the modeling computer requirements. A one-dimensional finite volume technique approach used in heat flux sensor analysis is used.⁹

The equation that describes one dimensional transient heat transfer is shown in Eq. (4), relating the rate of heating (or cooling) to the temperature gradient through the sensor probe body through the thermal diffusivity (α).

$$\partial T/\partial t = \alpha \cdot \partial^2 T/\partial x^2 \quad (4)$$

A fixed heat flux is assumed at the sensor body tip, and a fixed temperature at the base. If a structure is a layered structure, Eq. (4) holds within each layer and is subject to the additional requirement that the temperature and heat

flux of each layer's solution must be continuous at the interface between layers. In order to solve Eq. (4) numerically, each layer is divided into a number of *slices*, with a *node* at the center of each slice. It is at these nodes that the temperatures are calculated. Within a layer, where the properties are uniform, Eq. (4) is approximated by the set of Eqs. (5):

$$(T_{j,n+1}-T_{j,n})/\Delta t = \alpha_M (T_{j+1,n+1}-2T_{j,n+1}+T_{j-1,n+1})/\Delta x_2$$

alternately,

$$(-\alpha_M \Delta t / \Delta x_2) T_{j-1,n+1} + (1+2 \cdot \alpha_M \Delta t / \Delta x_2) T_{j,n+1} - (\alpha_M \Delta t / \Delta x_2) T_{j+1,n+1} = T_{j,n} \quad (5)$$

where α_M is the thermal diffusivity of layer M

Δt is the time increment

Δx is the distance between nodes

$j = 1, 2, \dots, j_{max}$ is the node number, starting with $j=1$ at the tip, $x=0$.

$n =$ the n th time step, with $n = 1$ at $t = 0$.

A more complex expression is required in order to maintain temperature and heat flux continuity for slices on either side of layers that have different material properties. Special algorithms exist for solving the set of Eqs. (5), which is unconditionally stable.¹⁰

For the sensor probe, two layers were used. A layer of platinum at the surface 1 μm thick was used to simulate the thin film thermocouple, and the other layer the 76 mm long stainless steel sensor body. Nodes in a slice in the platinum layer and 8.76 mm into the steel layer were chosen to report the time-temperature history.

Since the heat transfer coefficient for the bleed air chamber in the green run is not known, several model calculations were performed with different coefficients. The results, showing the modeled first 0.5 seconds of an instantaneous 300°C temperature increase on a 300°C sensor probe are given in Fig. 6 for the Au-Pt thin film thermocouple and Fig. 7 for the embedded Type K thermocouple.

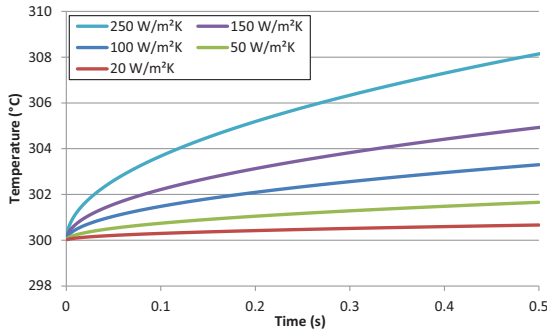


Figure 6. Results of numerical model showing time-temperature at the sensor probe tip for different heat transfer coefficients.

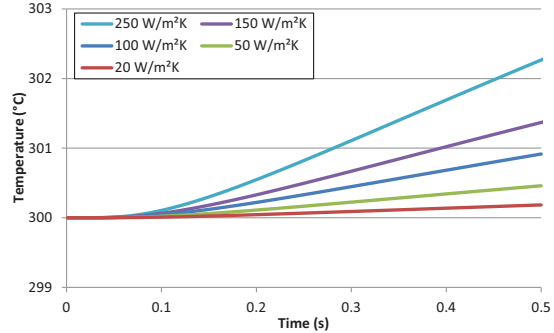


Figure 7. Results of numerical model showing time-temperature at the embedded thermocouple for different heat transfer coefficients.

To relate the numerical results to the green run data, the temperatures from the numerical model were used to calculate time constants using Eq. (1). For the calculations, the temperature differences over the 0.5 s range was used to calculate dT/dt , the temperature at 0.25 s was used for T , with $T_g = 600^\circ\text{C}$. The results for each heat transfer coefficient case are given in Table 1.

The modeled time constants were significantly large compared to the fit to the green run data. Also, the ratios of the modeled time constants were 0.275 where the green run data fit gives 0.0916. The air was modeled as pure dry air stagnant air and the sensor probe tip as a plane flush with the inside wall of the bleed air chamber, which was not the case in the green run. The turbulent flow of the bleed air may have caused the heat transfer coefficient to be larger than what was used in the numerical model. Also, the dissimilar shapes of Figs. 6 and 7 suggest that Eq. (1) may require more terms to fully characterize the time response of the embedded thermocouple.

Table 1. Time constants of the sensor probe for various heat transfer coefficients from the numerical model with the constants from the green run data fit for comparison.

Heat Transfer Coefficient (W/m ² K)	τ_1 (s)	τ_2 (s)	τ_2/τ_1
20	225.	815	0.277
50	90.2	326	0.276
100	45.1	164	0.276
150	30.0	109	0.275
250	18.1	66.0	0.274
<i>Green Run Data Fit</i>	2.40	26.2	0.0916

C. Bleed Air Temperature Derivation and Comparison

With a reaction time up to an order of magnitude less than the embedded type K probe, the thin film sensor alone gives a reliable indication of the gas temperature real-time. If the bleed air gas temperature is calculated with both thermocouples using Eq. (3), the noise contribution in the thermocouple readings significantly increases in the determination of the change rate in temperature \dot{T} , and causing significant uncertainty at times in calculating the gas temperature. To minimize those effects, frequency-domain fast Fourier transforms (FFT) of the temperature and rate data are used in Eq. (3) in place of the time-domain raw data. The inverse FFT of the result of this calculation gives the time-domain gas temperature less high frequency effects, in this case those greater than 2.238 kHz.

Figure 8 shows a comparison between the thin film and Type K raw thermocouple data of the scalloped region of Fig. 5 from the sensor probe and the gas temperature from FFT analysis, using the fitted time constants. The resulting derived gas temperature is less than 3.2°C higher than the thin film temperature sensor but up to 26°C higher than the embedded Type K thermocouple. As can be seen in Fig. 8, the thin film thermocouple gives a more accurate, higher fidelity indication of the actual gas temperature for real-time use than the embedded wire probe alone.

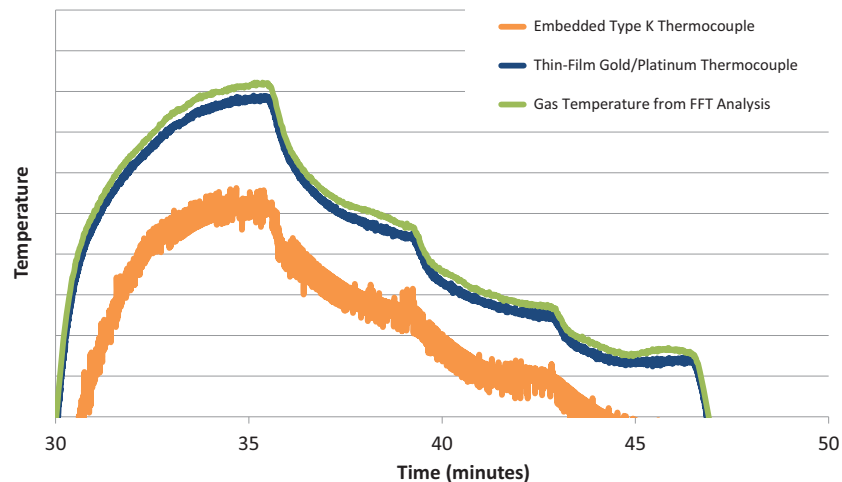


Figure 8. Close-up of the peak of the temperature curves from green run test showing calculated gas temperature relative to the thin-film and Type K thermocouple readings.

VI. Conclusions

As one of the objectives of the VIPR project, an experimental thin-film Au-Pt thermocouple sensor probe with a standard Type K embedded thermocouple was designed, fabricated and installed in a borescope port in the bleed air passage of a F117 turbofan engine during a green run. The sensor probe was fabricated from high temperature materials. Thin films of pure Au and Pt were sputter-deposited on the sensor probe tip rather than conventional thermocouple alloys to avoid separation of constituents during high temperature use.

The sensor probe and assembly were subjected to a strict protocol of multi-axis vibrational testing as well as elevated temperature pressure testing to be qualified for this application. A data acquisition unit to digitize the signals from the sensor probe for high accuracy and low noise measurements was designed and built as well. The acquired data demonstrated the fast response of the thin-film thermocouple as compared to a thermocouple probe, faster than expected from the numerical models. Deriving the bleed air gas temperature, the thin film thermocouple was seen to be within 3.2°C of the gas temperature.

Acknowledgments

The authors would like to thank those without whose effort would not make this work possible: Chuck Blaha of Jacobs Technology for the thin film depositions and wire bonding; Paul Solano of the GRC Mechanical & Rotating Systems Branch and Lawrence Kren of Vantage Partners for mechanical drawing support; Daniel Graf, Tracy Cantly, Greg Blank and the team at the GRC Fabrication Shop for machining the sensor body and parts; Richard Hanzel of Honeywell Technology Solutions, Inc. for assistance in pressure qualification tests; GRC Structural Dynamics Laboratory for performing vibration qualification tests; and the staff of the NASA GRC Test Facilities Operations, Maintenance, and Engineering (TFOME) organization in maintaining the fabrication and test equipment capabilities of the NASA GRC Microsystems Fabrication Lab.

The authors are grateful to Dr. Lawrence Matus, Chief of the Smart Sensors and Electronics Systems Branch of the NASA Glenn Research Center (GRC) for his review and comments on this work.

The authors would also like to thank Dr. John Lekki, Donald Simon and the GRC Aeronautics Research Office for supporting this effort and making the test possible. This work was sponsored by the Vehicle Systems Safety Technology (VSST) project of the Aviation Safety Program (AvSP) as part of NASA's Aeronautics Research Mission Directorate (ARMD). This work was performed at NASA Glenn Research Center with the F117 turbofan engine green run performed at Pratt & Whitney, East Hartford, CT.

References

¹ Wrbanek, J.D. and G.C. Fralick (2006), "Thin Film Physical Sensor Instrumentation Research and Development at NASA Glenn Research Center." NASA/TM—2006-214395; also as ISA# TP06IIS023.

² Engine make and model provided for information only and does not constitute an official endorsement, either expressed or implied, by NASA.

³ Simon, D.L. (2012), "Vehicle Integrated Propulsion Research (VIPR): Ground-test Maturation of Engine Health Management (EHM) Technology," *3rd Propulsion Control and Diagnostics Research Workshop*, February 28-March 1, 2012 (Cleveland, Ohio).

⁴ Burns, G.W., G.F. Strouse, B.M. Liu, B.W. Magnum (1992), "Gold versus Platinum Thermocouple: Performance, Data and an ITS-90 based Reference Function," NIST, Gaithersburg, MD, in *Temperature, Its Measurement and Control in Science and Industry*, Vol. 6, Ed. by J.F. Schooley (Amer. Institute of Physics, New York) 531–536.

⁵ Wilson, S.D., G.C. Fralick, J.D. Wrbanek, A. Sayir (2010), "Fabrication and Testing of a Thin-Film Heat Flux Sensor for a Stirling Converter." NASA/TM—2010-216063; also as AIAA-2009-4581.

⁶ Croarkin, M.C., W.F. Guthrie, G.W. Burns, M. Kaeser, G.F. Strouse (1993), "Temperature-Electromotive Force Reference Functions and Tables for the Letter-Designated Thermocouple Types Based on the ITS-90." NIST Monograph 175.

⁷ Forney, L.J. and G.C. Fralick (1994), "Two wire thermocouple: Frequency response in constant flow," *Rev. Sci. Instrum.* 65 (10) 3252-3257.

⁸ Forney, L.J. and G.C. Fralick (1995), "Multiwire thermocouples in reversing flow," *Rev. Sci. Instrum.* 66 (10) 5050-5054.

⁹ Fralick, G., J. Wrbanek, C. Blaha (2002), "Thin Film Heat Flux Sensor of Improved Design," NASA/TM—2002-211566.

¹⁰ Anderson, D.A., J.C. Tannehill, R.H. Pletcher (1984), *Computational Fluid Mechanics and Heat Transfer* (McGraw-Hill) 111.